PERGAMON

International Journal of Heat and Mass Transfer 41 (1998) 2735–2742

International Journal of HEAT and MASS TRANSFER

An analytical study for determining the dynamics of a boiling boundary in a channel

S. Benedek[a]*, D. A. Drew

Center for Multiphase Research, Rensselaer Polytechnic Institute, Troy, NY 12180-3590, USA
[a] *Institute for Electrical Power Research, 1251 Budapest, P.O.B. 80, Hungary*

Received 29 October 1996; revised 1 December 1997

Abstract

This paper applies control analysis techniques to study the response of two moving-boundary nodal models for the prediction of the time evolution of the boiling boundary in a heated channel. A model based on finite elements shows anti-resonances in the gain versus frequency curve similar to that of exact solution. The gain of the second model, based on a finite difference approach, has a damped variation with the frequency. This is the same with that of the conventional linearized fixed control volume model. The number of nodes to be used in a subcooled region is given for the models vs. frequency range of flow oscillation.

Nomenclature

c coefficient
d coefficient
h enthalpy [W s kg^{-1}]
f frequency [s^{-1}]
$F(s)$ transfer function
L length [m]
n number of node
N total number of nodes
Q heat added per unit mass [W kg^{-1}]
q'' heat flux [W m^{-2}]
s Laplace operator
t time [s]
u velocity [m s^{-1}]
z axial coordinate [m].

Greek symbols
Δ difference
ν traveling time [s]
ω angle velocity [1 s^{-1}]
σ time [s]
ρ density [kg m^{-3}].

Subscripts
boil boiling boundary
f saturated fluid
i inlet
n number of node
s saturated value
o steady state condition.

1. Introduction

A fundamental problem in heat transfer is the moving boundary problem in a boiling channel. The conventional method of solution uses fixed nodes, and calculates the enthalpy at each node. In this paper we consider moving node models, where the nodes are constrained to move so that the enthalpy change inside the nodes is constant. There are two versions of the moving node model. One, called the control volume model (or finite element model) [1–3], derives the equations for the motion of the nodes by assuming a linear enthalpy profile and integrating with respect to the space variable inside the nodes. We derive a new finite-difference model based on the assumption that the energy equation is satisfied at each node, using an approximation for the spatial derivative. Assuming constant pressure and incompressible phases, the momentum equation is decoupled from the energy and continuity equations and so can be ignored. For a known

* Corresponding author.

0017-9310/98 $19.00
PII: S0017-9310(98)00012-X

inlet velocity, the equations for the single-phase region of the boiling channel can be decoupled from the equations of the two-phase region.

The single-phase energy equation is linear, and therefore it can be solved by the Method of Characteristics (MOC) [4, 5].

In this paper using the results of [6], we investigate the time response of the two moving-boundary nodal models and we compare them with the solutions by the MOC and by the conventional fixed node model. We also apply linear control theory techniques to analyze the behavior of the models in the frequency domain to know better their general behavior in time.

2. Model

Assuming that the density and the system pressure are constant, the equation of conservation of mass becomes $\partial u/\partial z = 0$. This equation can be integrated to obtain $u = u_i(t)$. Then the enthalpy of a fluid moving in the single-phase region inside a heated channel (Fig. 1) is governed by the energy equation:

$$\frac{\partial h}{\partial t} + u_i(t)\frac{\partial h}{\partial z} = Q \tag{1}$$

where Q is assumed to be constant and uniform in each element.

2.1. Control volume (Finite element) model

Consider the region of the channel: $L_{n-1}(t) \leqslant z \leqslant L_n(t)$, where the axial position $L_n(t)$ is defined as the location inside the channel where the liquid reaches a value of enthalpy equal to $h_n = h_i + [(h_f - h_i)/N]n$. (In Fig 1. $N = N_s$ where the enthalpy reaches its saturated value h_f at L_{N_s} or $L_{boil,0}$.) This enthalpy, h_n, is taken to be constant. Integrating equation (1) over this region and applying Leibnitz's rule we obtain:

$$\frac{\mathrm{d}}{\mathrm{d}t}\int_{L_{n-1}(t)}^{L_n(t)} h(z)\,\mathrm{d}z - h(L_n)\frac{\mathrm{d}L_n}{\mathrm{d}t} + h(L_{n-1})\frac{\mathrm{d}L_{n-1}}{\mathrm{d}t}$$

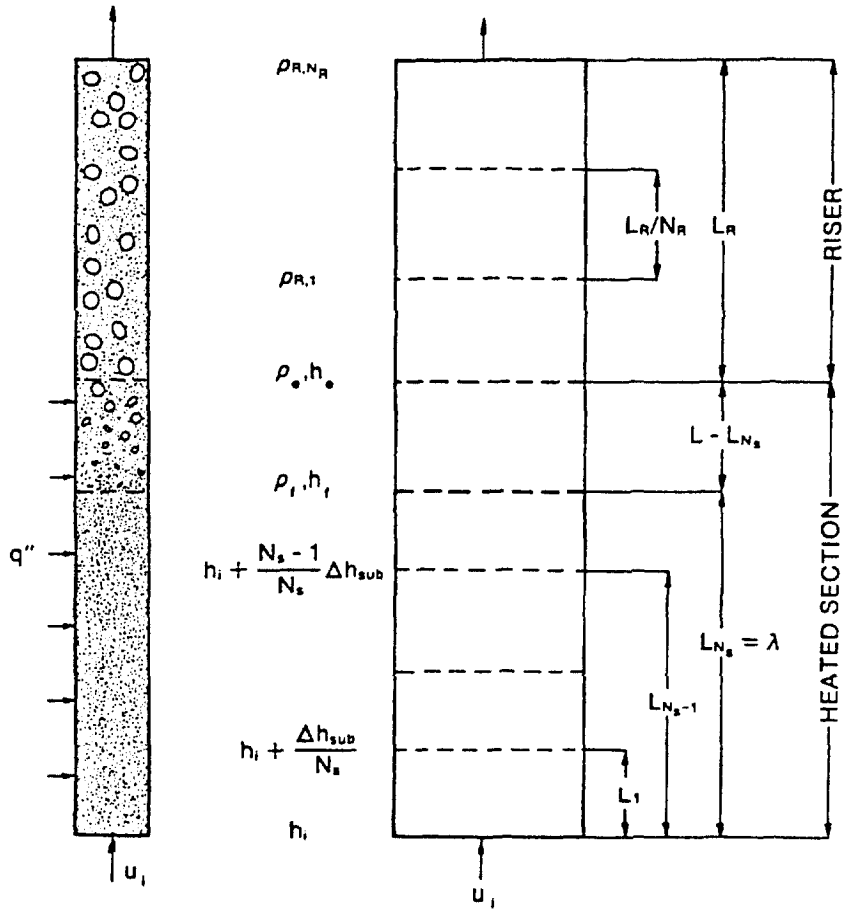

Fig. 1. Schematic of the vertical heated channel.

$$+u_i[h(L_n)-h(L_{n-1})] = Q(L_n-L_{n-1}). \quad (2)$$

Approximating the integral by assuming that h is piecewise linear in the segment $L_{n-1} \leqslant z \leqslant L_n$ we can evaluate the remaining integral. Thus the equation for the control volume model is

$$\frac{dL_n}{dt} = 2u_i - 2\frac{Q}{(h_n-h_{n-1})}(L_n-L_{n-1}) - \frac{dL_{n-1}}{dt}. \quad (3)$$

2.2. Finite difference model

The second nodal model (finite difference model) is derived by writing the time derivative of the enthalpy at the boundary of the node. Since the boundary of the node follows the position inside the channel with a given value of enthalpy, we can write:

$$\frac{dh_n}{dt} = 0 = \left.\frac{\partial h}{\partial t}\right|_{z=L_n} + \left.\frac{\partial h}{\partial z}\right|_{z=L_n}\frac{dL_n}{dt}. \quad (4)$$

Substituting $\partial h/\partial t$ from equation (1) and approximating the derivative by

$$\frac{\partial h}{\partial z} \cong \frac{h_n-h_{n-1}}{L_n-L_{n-1}} \quad (5)$$

we obtain:

$$\frac{dL_n}{dt} = u_i - \frac{Q}{(h_n-h_{n-1})}(L_n-L_{n-1}). \quad (6)$$

2.3. Fixed node model (Method of lines)

Using an upwind Euler integration the energy equation for $h(z_n, t) = h_n(t)$ can be written as

$$\frac{dh_n}{dt} = Q - u_i\frac{\partial h}{\partial z} \cong Q - u_i\frac{h_n-h_{n-1}}{L_n-L_{n-1}}. \quad (7)$$

For comparison with the other models, note that the position of the boiling boundary (in the node $n = N_v$) is approximately,

$$L_{boil} \cong L_{n-1} + \frac{L_n-L_{n-1}}{h_n-h_{n-1}}(h_f-h_{n-1}). \quad (8)$$

2.4. Exact solution—Method of characteristics

The exact solution for equation (1) (Q is constant) is given by [4, 5]:

$$\frac{dh}{d\sigma} = Q \quad (9)$$

$$\frac{dt}{d\sigma} = 1 \quad (10)$$

$$\frac{dz}{d\sigma} = u_i(t). \quad (11)$$

Note that $h = h_f = Q\sigma + h_i$, so that boiling occurs when $\sigma = v = [(h_f-h_i)/Q][= (L_{boil,0}/u_{i0})]$. The solution for $z(\sigma)$ is

$$z(\sigma) = \int_0^\sigma u_i[t(\sigma)]\,d\sigma. \quad (12)$$

Changing variable to t, and noting that for $z = L_{boil}$, $\sigma = 0$ corresponds to time $t-v$, we have

$$L_{boil} = \int_{t-v}^{t} u_i(t')\,dt'. \quad (13)$$

Then

$$\frac{dL_{boil}}{dt} = u_i(t) - u_i(t-v). \quad (14)$$

3. Analysis

The two moving boundary nodal methods give sets of ordinary differential equations (ODEs) for the position of the nodes $L_1, L_2, \ldots, L_N$. The conventional upwind difference equations give a set of ordinary differential equations for the enthalpies at the fixed nodes. For comparison, the position of the boiling boundary must be interpolated. The exact solution gives the enthalpy at all space points, at all times.

The form of the solution for the moving boundary nodal methods allows the direct application of control theory techniques [7, 8] to study the response of the system as a function of the frequency of the inlet velocity, which appears as 'forcing' in these equations. In the exact solution, also, equation (14) is amenable to control techniques. However, these techniques cannot be applied directly to the method using fixed nodes. Here we linearize the system about the steady-state and study the response to small periodic velocity fluctuations.

3.1. Frequency domain analysis

We use the Laplace transformation in the $s = i\omega$ domain. The flow chart of the systems are presented in Figs. 2 and 3. The gain of the system is defined as the ratio between the amplitude of the response of the system, $\Delta L_n(s)$, and the amplitude of the perturbed forcing function, $\Delta u_i(s)$.

The transfer function of control volume model [equation (3)] is calculated by:

$$\Delta L_n(s) = \{\Delta L_{n-1}(s)(c-s) + 2\Delta u_i(s)\}\frac{1}{s+c}. \quad (15)$$

By substituting for $n = 1, 2, \ldots$, we obtain

$$F(s) = \frac{\Delta L_n(s)}{\Delta u_i(s)} = 2\left[\frac{(c-s)^{n-1}}{(s+c)^n} + \frac{(c-s)^{n-2}}{(s+c)^{n-1}} + \cdots + \frac{1}{s+c}\right] \quad (16)$$

where:

$$c = \frac{2u_{i0}}{L_{boil,0}}N \quad (c = 2N/v)$$

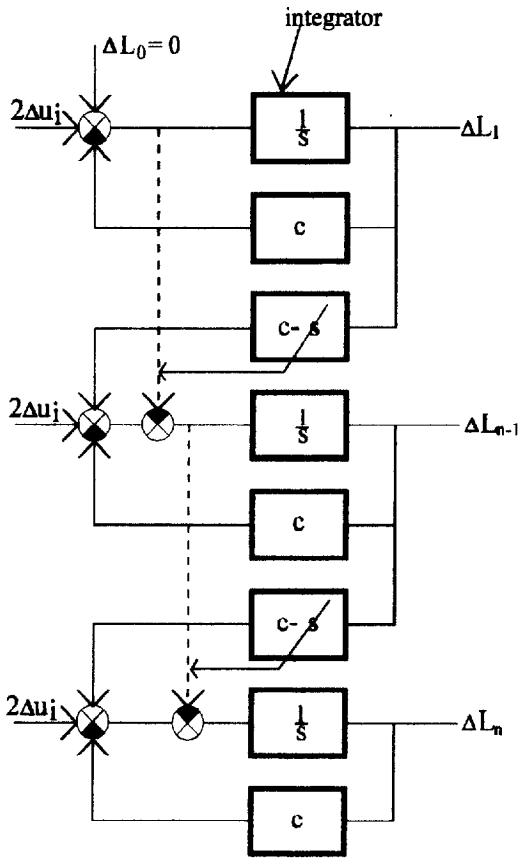

Fig. 2. Flow chart of the system. Control volume (finite element) model [equation (3)].

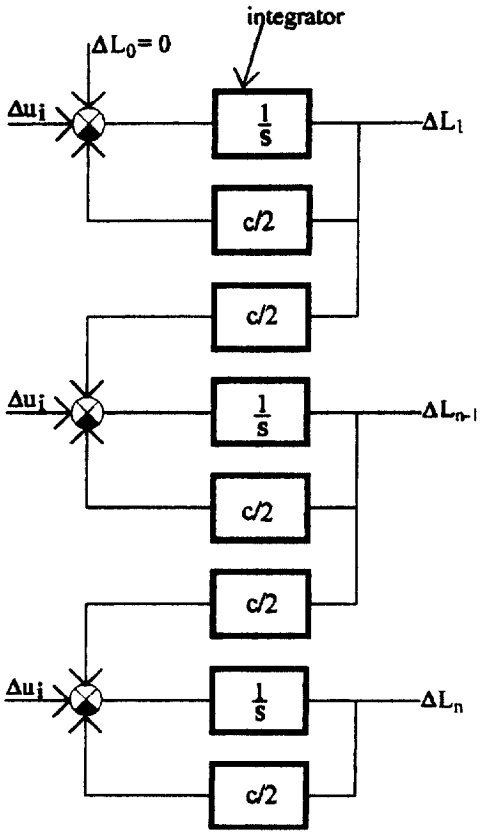

Fig. 3. Flow chart of system. Finite difference model [equation (6)].

and assuming, $u_{i0} = 0.3$ m s^{-1}, $L_{boil,0} = 2.7$ m, $Q = 5200$ W kg^{-1}, $h_f = 4.468 \times 10^5$ and $h_i = 4 \times 10^5$ W s kg^{-1} and so $v = 9$ s.

The transfer function of finite difference model [equation (6)] is calculated by:

$$\Delta L_n(s) = \{\Delta L_{n-1}(s)c/2 + \Delta u_i(s)\}\frac{1}{s+c/2}. \tag{17}$$

Again, substituting for $n = 1, 2, \ldots$, we have

$$F(s) = \frac{\Delta L_n(s)}{\Delta u_i(s)} = \left[\frac{(c/2)^{n-1}}{(s+c/2)^n} + \frac{(c/2)^{n-2}}{(s+c/2)^{n-1}} + \cdots + \frac{1}{s+c/2}\right]. \tag{18}$$

The transfer function of linearized fixed node model [equations (7) and (8)] is calculated (in the node $n = N_c$) by:

$$\Delta L_{boil}(s) \cong \frac{L_n - L_{n-1}}{h_n - h_{n-1}}[-\Delta h_{n-1}(s)] = \frac{u_i}{Q}[-\Delta h_{n-1}(s)] \tag{19}$$

$$\Delta h_n(s) = \{\Delta h_{n-1}(s)c/2 + d_n \Delta u_i(s)\}\frac{1}{s+c/2} \tag{20}$$

$$F(s) = \frac{\Delta L_{boil}(s)}{\Delta u_i(s)} \cong \left[\frac{(c/2)^{n-1}}{(s+c/2)^n} + \frac{(c/2)^{n-2}}{(s+c/2)^{n-1}} + \cdots + \frac{1}{s+c/2}\right] \tag{21}$$

where:

$$d_n = \frac{h_{n-1} - h_n}{L_n - L_{n-1}}.$$

We take fixed uniform nodes, so that $d_n = d$ is independent of n. The flow chart of the fixed node model has a similar structure as that of the finite difference model (see Fig. 3). The transfer function of exact solution [equation (14)] is calculated by:

$$F(s) = \frac{\Delta L_{boil}(s)}{\Delta u_i(s)} = \frac{1 - e^{-vs}}{s}. \tag{22}$$

This function has the first zero gain value less than 0.01 (i.e. 40 dB) at $f_1 = 1/v$ and the others are $f_i = i/v$ and $i = 2, 3, \ldots \infty$. The gain is v when $s \to 0$ or $t \to \infty$

(if $v = 9$ s, the gain is 19 dB, see Fig.4). When $s \to \infty$ or $t \to 0$ the gain will be zero, i.e. ∞ dB.

After some manipulation of equation (16), we have:

$$\frac{\Delta L_N(s)}{\Delta u_i(s)} = \frac{1-\left(\frac{c-s}{c+s}\right)^N}{s} \tag{23}$$

with using

$$\lim_{N\to\infty}\left(1+\frac{z}{N}\right)^N = e^z,$$

we see that the transfer function approaches that of the exact solution as $N \to \infty$:

$$\lim_{N\to\infty}\frac{\Delta L_N(s)}{\Delta u_i(s)} = \frac{1-e^{-vs}}{s}. \tag{24}$$

Again after some manipulation of equations (18) and (21) we have:

$$\lim_{N\to\infty}\frac{\Delta L_N(s)}{\Delta u_i(s)} = \frac{1-e^{-vs}}{s}. \tag{25}$$

Thus both moving volume models and the fixed node model converge to the exact solution [equation (22)]. All the transfer functions give stable behavior of the systems as the real parts of the roots of denominators of these functions are negative, including one possible zero value in [equation (22)].

3.2. *Time domain analysis*

The behavior discussed in Section 3.1 can be also observed in the time domain. In general case, the simulation of different models can be carried out by numerical integration for the analysis.

The exact solution can be obtained from the method of characteristics [equations (9), (10), (11)]. The position of the traveling enthalpy wave is $z = u_i t$. Below this line, the characteristics come from boundary, above this line, they come from initial conditions.

Enthalpy is determined:

if $z < u_i t$

$$h(z,t) = Q\left(\frac{z}{u_i}\right) + h_1 + h_3\left(t-\frac{z}{u_i}\right) \tag{26}$$

if $z > u_i t$

$$h(z,t) = Qt + h_1 + h_2(z-u_i t) \tag{27}$$

where:

$$h_2 = \frac{\partial h}{\partial z} = \frac{Q}{u_{i0}}, \quad h_3 = \frac{\partial h_1}{\partial t}.$$

4. Results

4.1. *Results in frequency domain*

It can be shown that the control volume model the finite difference model and the fixed node model approach the exact solution as $N \to \infty$. Still, it is important to be able to compute with a small number of nodes to attain a certain degree of approximation.

Next, the behavior of different models will be studied, a comparison between the control volume (finite element) model [equations (3) and (15)], the finite difference model [equations (6) and (17)] and the exact solution [equations (14) and (22)] for ten nodes is shown in Fig. 4. The behavior of the fixed node model [equations (7), (8) and (19)] is very similar to that of the finite difference model.

It can be seen in Fig. 4, that for two moving boundary models, the gains are practically the same below the first antiresonant frequency $f_1 = 0.115$ Hz (with zero gain, that means practically less than 0.01, i.e. 40 dB). The gains calculated by exact solution verify these results, see Fig.4. Below the first antiresonant frequency the number of nodes can be chosen as $3 \leqslant N \leqslant 10$ for the subcooled region.

In the neighborhood of the first (f_1) and higher frequencies ($f_i = i/v$ and $i = 2, 3, \ldots \infty$) the behavior of the models will be different. The gain for the control volume model shows an antiresonant behavior (with zero gains) similarly to that of exact solution. The antiresonant effects with zero gains are caused by the negative sign of the last term on right side in equation (3).

In spite of this the finite difference (and fixed node) models give damped curve, see Fig. 4. With $N = 200$ nodes a small oscillation (but without zero values) of gains of finite difference (and fixed node) model [equation (6)] can be observed only in the small range of frequencies

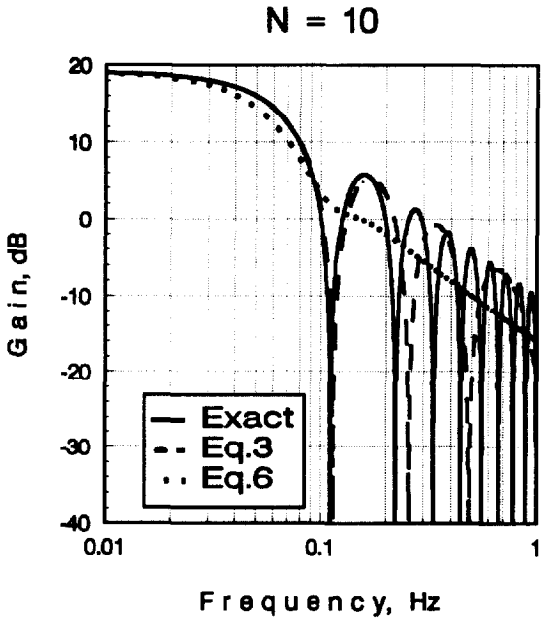

Fig. 4. Gain vs frequency. Control volume model [equation (3)], finite difference model [equation (6)] and the exact solution.

from f_1 to $6*f_1$, see in Fig. 5. On the contrary, the exact solution gives an antiresonant behavior (with zero gains) for whole higher frequency range. The finite difference and the fixed node models would yield similar response if $N \geqslant 10\,000$ nodes were used.

The behavior of control volume model [equation (3)] compared with exact solution can be seen in this interesting region in Fig. 6. For ensuring 10 % error in the places of antiresonant frequencies between the exact solution and the control volume model, following number of nodes should be chosen, in the region of f_1, $N = 10$, between f_1 and $3*f_1$, $N = 20$ and between $3*f_1$ and $6*f_1$, $N = 30$. For achieving 2% error in the last frequency range, $N = 100$ should be used.

4.2. Results in time domain

The different behavior discussed in last section can be also observed in the time domain. In a numerical example, we selected the first antiresonant frequency, $f_1 = 0.115$ Hz (for $N = 10$) of the control volume model [equation (3)] where the finite difference model [equation (6)] and the fixed node model [equation (8)] have a gain about 1.2 (i.e. 1.6 dB) (see in Fig. 4). After sinusoidal perturbation of inlet fluid velocity [$(u_i = 0.3 + 0.1* \sin(2\pi ft)$], the changes in length of boiling boundary vs. time can be seen in Fig. 7. The changes (0.12 m to 0.1 m s^{-1}) in time using models [equations (6) and (8)] are equivalent to gain of 1.6 dB. Using control volume model [equation (3)] (with zero gain) no changes in position occurred, what is correct. (The exact solution has also zero gain at this frequency, see in Fig. 4.)

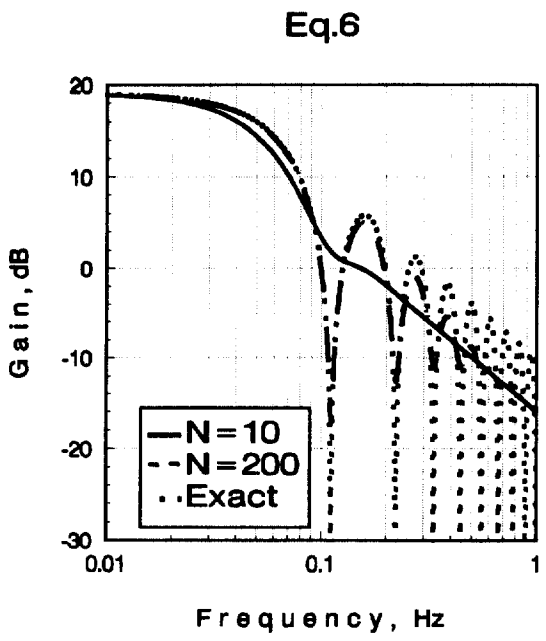

Fig. 5. Gain vs. freqency. Finite difference model [equation (6)] at different number of nodes compared to exact solution.

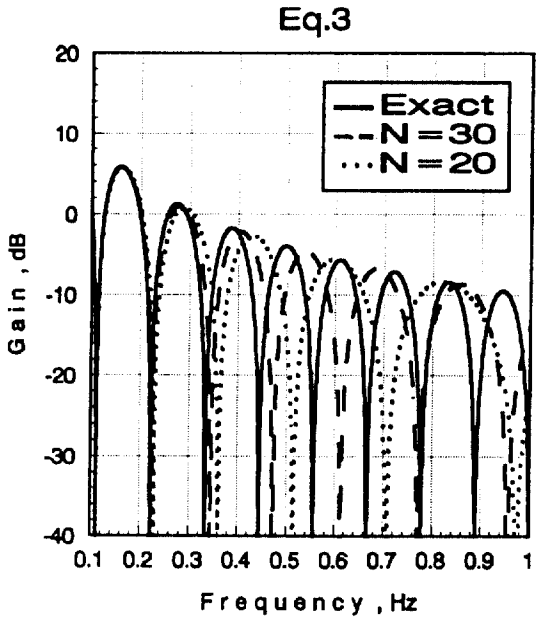

Fig. 6. Gain vs. freqency. Control volume model [equation (3)] at different number of nodes compared to exact solution.

Another interesting case to study is the behavior of the models when a step change in the inlet velocity is imposed. We calculated the time evolution of the boiling boundary with an inlet velocity of $u_{i0} = 0.3$ m s^{-1} when $t < 0$, and $u_i = 0.21$ m s^{-1} when $t > 0$ and $N = 10$ nodes. Figure 8 shows that the solution obtained from the control volume model, [equation (3)], yields a quicker response than those from [equations (6) and (8)] when compared with the exact solution. A step change contains all frequencies (but weighted), therefore similar evolutions of boiling boundary will be yielded. The gain of transfer functions is v ($v = 9$ s or 19 dB) when $s \to 0$, $t \to \infty$, in Fig. 4. In this way if the change of u_i is 0.09 m s^{-1}, then the change of L_{boil} will be $9*0.09 = 0.81$ m which is checked by the simulation. Note that the new steady state value of boiling boundary will be achieved in $v = 9$ s.

Figure 9 shows the evolution of the enthalpy inside the channel in time using exact solution [equations (26), (27)] after the same change in the inlet velocity as above and assuming $h_3 = 0$. It can be seen that the enthalpy of the saturated fluid $h_f = 446\,800$ W s kg^{-1} will be the same in the new steady state in $t \geqslant 9$ s, while the steady boiling boundary will change from $L_{boil,0} = 2.7$ m to $L_{boil} = 1.89$ m. The exact solution (in Fig. 8) yields from this surface (Fig. 9) cutting by the plane of $h = h_f$. The calculated surface is correct below this plane (i.e. only in the subcooled region).

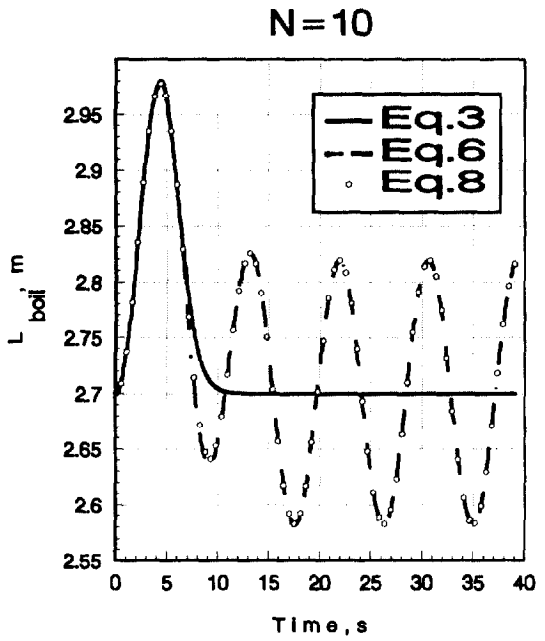

Fig. 7. Time evolution of change of the boiling boundary after a periodic perturbation of the inlet velocity. (Control volume model [equation (3)], finite difference model [equation (6)] and fixed node model [equation (8)]).

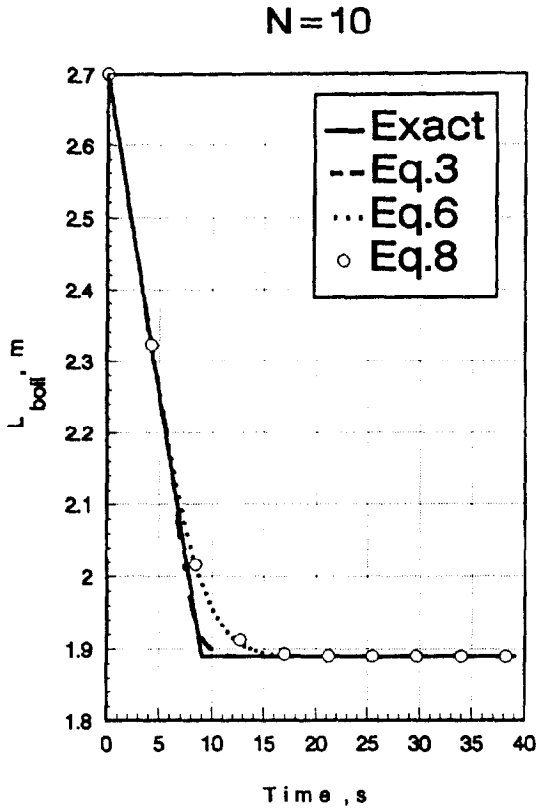

Fig. 8. Time evolution of the boiling boundary after a step perturbation in the inlet velocity. (Control volume model [equation (3)], finite difference model [equation (6)], fixed node model [equation (8)] and the exact solution [equations (26), (27)]).

Thus the results in frequency and time domains got from different methods have been verified by each other.

5. Conclusions

Two, a control volume model (with finite elements) and a finite difference models with moving boiling boundary have been analyzed in comparison to the conventional (linearized) fixed node model and to the exact solution method. The investigations have been carried out in the frequency domain and in the time domain with periodic perturbations and with a step change of the inlet fluid velocity. These results compared well with each other.

The behavior of the conventional (linearized) fixed node model is practically the same as that of the finite difference model in the whole range of frequency.

The behavior of the finite element, of the fixed node and of the finite difference models, and of the exact solution are the same at lower frequencies, where the number of nodes in the subcooled region can be chosen between $N = 3$ and $N = 10$. After the first antiresonant frequency of the system, the behavior of these models will differ from each other. The first 'critical' frequency ($f_1 = 1/v = Q_f/(h_f - h_i) = u_{in}/L_{boil,0}$) is physically the reciprocal value of fluid traveling time (as a delay) to boiling boundary in the heated channel. Above this frequency (approx. ~0.1–0.2 Hz) only the control volume model (with finite elements) with moving boiling boundary is a practical method for approximating the exact solution (with zero gains) using some number of nodes $10 \leqslant N \leqslant 30$. The finite difference and fixed node models give only a damped gain curve without antiresonant effects for whole frequency region, using $3 \leqslant N \leqslant 10$. The finite difference model (with moving boiling boundary) and the fixed node model converge much slower (with increasing of number of nodes) than the control volume model (with moving boiling boundary) to the exact solution over the first 'critical' frequency.

Fundamentally, the gains (the behavior of the system) are determined by value of v in whole range of frequency.

To our knowledge, no experimental results exist for comparison with the model predictions. The presence of the antiresonance behavior in all the models suggests that measurements should be made and compared to the analytic predictions.

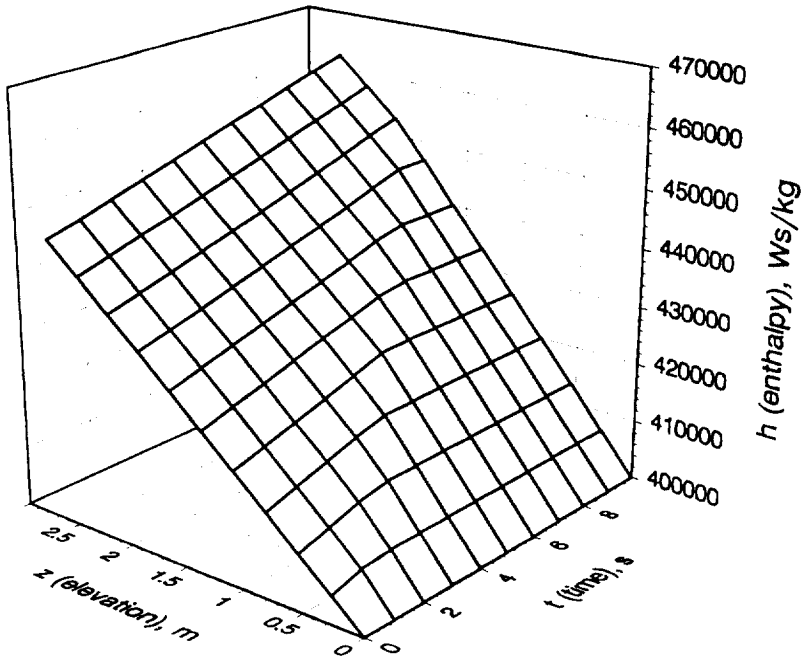

Fig. 9. Time and spatial evolution of the boiling boundary after a time step perturbation in the inlet velocity.

Acknowledgment

This work was sponsored partially by the Hungarian National Foundation for Scientific Research (Grant T 022396).

References

[1] Takenaka N, Lahey RT Jr, Podowski MZ. The analysis of chaotic density-wave oscillations. Transactions of the ANS, 1991;63:197.

[2] Lahey RT Jr *et al.* Chaotic phenomena in density-wave oscillations. Int Symp on New Basis for Engineering Science—Algorithms, Dynamics and Fractals, Okayama, Japan, Nov. 23–8, 1992, 21–64.

[3] Chang CJ. The analysis of chaotic instabilities in boiling systems. Ph.D Thesis, 1994, Rensselaer Polytechnic Institute, Troy, U.S.A.

[4] Lahey RT, Moody FJ. The thermal hydraulics of a boiling water nuclear reactor. LaGrange Park, American Nuclear Society, 1977.

[5] Moody FJ. Introduction to Unsteady Thermofluid Mechanics. New York: John Wiley & Sons Inc., 1990.

[6] Benedek S, Garea VB, Lahey RT Jr, Drew DA. Optimal model for determining the dynamics of a boiling boundary in a channel. Proc of AIChE Annual Meeting, Miami Beach Nov. 12–17, 1995.

[7] Kuo BC. Automatic Control Systems. Englewood Cliffs, New Jersey: Prentice-Hall Inc., 1991.

[8] Csáki F. State Space Methods for Control Systems. Budapest: Akademia P.C., 1977.